HHS Public Access

Author manuscript

J Immunol. Author manuscript; available in PMC 2019 October 01.

Published in final edited form as:

J Immunol. 2018 October 01; 201(7): 1994–2003. doi:10.4049/jimmunol.1800235.

Impaired development and expansion of germinal center follicular T helper cells in SIV-infected neonatal macaques

Huanbin Xu, **Widade Ziani**, **Jiasheng Shao**, **Lara A. Doyle-Meyers**, **Kasi E. Russell-Lodrigue**, **Marion Ratterree**, **Ronald S. Veazey**, and **Xiaolei Wang**[*]

Tulane National Primate Research Center, Tulane University School of Medicine, 18703 Three Rivers Road, Covington, LA 70433

Abstract

Germinal center follicular CD4+ T helper (GC Tfh) cells are critical for cognate B-cell help in humoral immune responses to pathogenic infections. Although Tfh cells are expanded or depleted in HIV/SIV-infected adults, the effects of pediatric HIV/SIV infection on Tfh cells remain unclear. Here we examined changes in lymphoid follicle formation in lymph nodes focusing on GC Tfh, B-cell development and differentiation in SIV-infected neonatal rhesus macaques (*Macaca mulatta*) compared with age-matched cohorts. Our data showed that follicles and GC of normal infants rapidly formed in the first few weeks of age, in parallel with increasing GC Tfh cells in various lymphoid tissues. In contrast, germinal center development and GC Tfh cells were markedly impaired in SIV-infected infants. There was a very low frequency of GC Tfh cells throughout SIV infection in neonates and subsequent infants, accompanied by high viremia, reduction of B-cell proliferation/resting memory B-cells, and displayed proinflammatory unresponsiveness. These findings indicate neonatal HIV/SIV infection compromises the development of GC Tfh cells, likely contributing to ineffective antibody responses, high viremia, and eventually rapid disease progression to AIDS.

Keywords

Lymph node; Follicle; Follicular CD4 T helper cells; SIV; Neonates; pediatric AIDS; HIV

Introduction

At birth, the newborn infant undergoes a rapid transition from the “sterile” environment of the womb to an external surrounding with abundant foreign antigens, and thus immune development and responses must be prepared to immediately cope with the plethora of foreign antigens suddenly encountered (1). Although neonatal and infant immune systems are thought to be functionally “immature” (1), it has been reported that broadly neutralizing

[*]Corresponding author: Tulane National Primate Research Center, Division of Comparative Pathology, 18703 Three Rivers Road, Covington, LA 70433 USA, Phone (985) 871-6618, Fax: (985) 871-6510, xwang@tulane.edu.

Author Contributions: H.X. analyzed most of the experiments and wrote the manuscript; W.Z., J.S., D.L., R.K., and M.L., helped to complete experiments; X.W. performed confocal microscopy; H.X., X.W. and R.S.V. designed the experiments and prepared the manuscript.

Conflict-of-interest disclosure: The authors declare no competing financial interests.

antibodies (bnAb) against HIV can develop quickly in infants (2). Further, our previous studies showed that CD4+ T cells in mucosal tissues of newborn macaques have a "memory" phenotype, and higher rates of proliferation than adults. These cells are the primary targets for early HIV/SIV replication in infants, which may be the reason infants have markedly higher and more sustained levels of viral replication than HIV-infected adults (3, 4).

In neonates, organized lymphoid tissues are not fully developed, and early immune protection initially relies on IgG antibodies of maternal origin, levels of which decline after birth, with a half-life of 21–30 days (5). Once exposed to antigens, naïve B cells are initially primed, and then migrate to the border of the T cell and B cell zones where they proliferate and form stable interactions with antigen-specific T cells to become fully activated (6, 7). A pool of antigen-specific B cells with the highest relative affinity then gain access to the newly forming germinal centers (GCs) (8–11), further proliferate, undergo random Ig somatic hypermutation (SHM), and rearrange and diversify their IgV genes, resulting in mutant GC B cell clones with a broad repertoire of potentially neutralizing antibodies (12, 13), and generation of high-affinity antibody-secreting plasma cells and long-lived memory B cells (14–18). The germinal center (GC) reaction that occurs in organized lymphoid tissues including lymph nodes, spleen, and mucosa-associated lymphoid tissues are critical for developing effective humoral immune responses. Within mature GCs, signaling from GC Tfh cells, such as CD40, IL-4, IL-9, IL-21 and ICOS, play a pivotal role in the GC reaction during intermittent cognate engagements between GC B and Tfh cells (19–21). These GC Tfh and B cell interactions facilitate several re-iterative rounds of B cell mutation and selection, result in the terminal differentiation and generation of memory B cells and plasma cells secreting high affinity antibodies (15, 22).

Tfh cells provide help for cognate B-cell maturation, and promote potent primary antibody responses to infections (14, 23). Absence of Tfh cell help results in B-cell apoptosis, and prevents B cell differentiation and development of effective humoral immune responses (24). We previously reported that GC Tfh cells, defined as CXCR5+PD-1^{HIGH} CD4+ T cells in GC of follicles in macaques (25), are expanded in asymptomatic stages of SIV infection, yet are depleted in adults with AIDS. These Tfh cells harbored within what has been referred to as "sanctuary sites" have also been reported to be major reservoirs of HIV (26–28), and infected Tfh cells have been linked with abnormal B-cell responses (29–33).

Notably, more rapid disease progression and higher mortality rates are observed among HIV/SIV infected infants than adults (34). However, the effects of SIV infection on Tfh cells in developing neonates are still unknown. Understanding aspects of the pathogenesis of HIV infection that are unique to neonates and young children are essential for optimizing prevention and treatment strategies for pediatric HIV patients.

Here, we examined the development of lymph node follicle formation in normal and SIV-infected neonatal macaques. We monitored dynamics of GC Tfh cell development, and analyzed levels of viral loads and proinflammatory responses in plasma of SIV-infected neonates, compared with age-matched neonatal cohorts throughout neonatal development. The results showed that lymphoid follicles in organized lymphoid tissues of normal neonates

rapidly developed in the first few weeks after birth. However, in contrast to age-matched controls, SIV infection in newborns resulted in marked impairment of lymphoid follicle development, abrogation of germinal center development, and eventually, complete obliteration of normal lymphoid tissue architecture. We also show severely impaired GC development with significantly fewer numbers of GC Tfh cells, and impaired proliferation of B cells from lymph nodes of infants, accompanied by high viremia, yet decreased proinflammatory responses that are typical of primary infection in adults. These findings suggest SIV infection in newborn prevents GC Tfh cell development and differentiation, resulting in rapid impairment of humoral immune responses, which likely contributes to the accelerated disease progression in pediatric hosts.

Materials and Methods

Ethics statement

All animals in this study were housed at the Tulane National Primate Research Center in accordance with the Association for Assessment and Accreditation of Laboratory Animal Care International standards. All studies were reviewed and approved by the Tulane University Institutional Animal Care and Use Committee. Animal housing and studies were carried out in strict accordance with the recommendations in the Guide for the Care and Use of Laboratory Animals of the National Institutes of Health (NIH, AAALAC #000594) and with the recommendations of the Weatherall report; “The use of non-human primates in research”. All clinical procedures were carried out under the direction of a laboratory animal veterinarian. All procedures were performed under anesthesia using ketamine or tiletamine/zolazepam, and all efforts were made to minimize stress, improve housing conditions, and to provide enrichment opportunities (e.g., objects to manipulate in cage, varied food supplements, foraging and task-oriented feeding methods, interaction with caregivers and research staff).

Animals and virus

In this study, total of 85 Indian-origin rhesus macaques (*Macaca mulatta*; RMs) were utilized to examine Tfh cells and other cell subsets from lymph nodes. The ages of infant macaques were characterized as previously reported (35) as: neonate (0–1 month); infant (1~6 months), juvenile (6 months~3yrs) and adult (> 3yrs). Infant animals were intravenously inoculated with SIVmac251 (100 TCID50) either at birth (n=28) or at 4-months of age (n=6). Lymph nodes were collected at day 0, 3, 7, 14, 21, 28 and month 2–3 post SIV infection. The animals grouped based on specific timepoints after early SIV infection, but chronically infected infants that developed illnesses attributed to AIDS were combined since all infected infants developed clinical signs within 2–3 months of infection. Tissues from SIV naive, age-matched neonates/infants (n=35) and adults (n=16, from 3–12 years of age) were examined as controls. Numbers of animals and tissues used for individual experiments are provided in the figure legends.

Tissue collection and phenotyping

Blood and lymph nodes were collected at necropsy from uninfected controls, or in acute (7–28 days), or AIDS animals with defined opportunistic infections and/or neoplasm/

lymphoma. Lymph nodes were collected and fixed in formalin, frozen for immunohistochemistry to detect specific lymphocyte subsets in situ, and another section was processed into viable single cell suspensions for flow cytometry. Plasma was collected to monitor viral loads and cytokine/chemokine responses.

Flow cytometry for surface and intracellular antigens was performed on viable cell suspensions using standard protocols (36). Cells were stained with: CD3 (SP34), CD4 (SK3), CD20 (2H7), CXCR5 (MU5UBEE, eBioscience), PD-1 (EH12.2H7, BioLegend), Ki67 (B56), IgD (Southern Biotech), CD27 (O323, BioLegend) and LIVE/DEAD Fixable Aqua Dead Cell Stain Kit (Invitrogen, Grand Island, NY). All antibodies and reagents were purchased from BD Biosciences Pharmingen (San Diego, CA) unless otherwise noted. Isotype-matched controls were included in all experiments. After staining, samples were resuspended in BD Stabilizing Fixative (BD Biosciences) and acquired on a FACS FORTESSA (Becton Dickinson, San Jose, CA). Data were analyzed with Flowjo software (Tree Star, Ashland, OR).

Multi-color confocal microscopy analysis and immunohistochemistry

Lymph node tissues were processed for immunohistochemistry as previously described (37). In brief, tissues were fixed in formalin, embedded in paraffin, sectioned and stained as below. Other sections were snap frozen in optimum cutting temperature compound (OCT) and 7 μm frozen sections were stained using unconjugated primary antibodies including CD20, PD-1, and CD68, followed by appropriate secondary antibodies conjugated to the fluorescent dyes Alexa 488 (green), Alexa 568 (red) or Alexa 633 (blue) (Molecular Probes, Eugene, OR). Confocal microscopy was performed using a Leica TCS SP2 confocal microscope equipped with three lasers (Leica Microsystems, Exton, PA). Individual optical slices representing 0.2 μm and 32 to 62 optical slices were collected at 512 × 512 pixel resolution. NIH Image (version 1.63, Bethesda, MD) and Adobe Photoshop CS5 (San Jose, CA) were used to assign colors to the channels collected. To detect PD-1+, CD20+, or CD68+ cells in lymph nodes by immunohistochemistry, paraffin-embedded sections were deparaffinized, and antigens were unmasked using high-temperature antigen retrieval by heating slides in a steam bath chamber (Flavor Scenter Steamer Plus; Black and Decker, Hunt Valley, MD) with 0.01 M citrate buffer pH 6.0 for 20 minutes. Slides were then cooled, washed twice in phosphate-buffered saline (PBS), and blocked with peroxidase blocking reagent (Dako, Glostrup, Denmark) for 10 minutes, washed again in PBS, and further blocked with serum-free protein block (Dako) for 30 minutes. Sections were then incubated with the purified anti-PD-1, CD20, or CD68 Ab for 1 hour at room temperature, washed (PBS), and developed using a Vectastain ABC peroxidase kit (Vector Laboratories, Burlingame, CA) and 3,3-diaminobenzidine DAB (Biocare Medical, Concord, CA).

Detection of SIV-infected cells in lymph nodes

To identify numbers and distribution of productively-infected cells in lymph nodes of chronically SIV-infected macaques, a nonradioactive *in situ* hybridization for viral RNA was performed on formalin-fixed, paraffin-embedded sections of mesenteric lymph nodes as previously described (35). Briefly, 5-μm sections were cut and adhered to silanized glass slides. After deparaffinization in xylene, rehydration in PBS, and antigen retrieval with

steam, sections were acetylated and hybridized with digoxigenin-labeled antisense SIV riboprobes (Lofstrand Labs, Gaithersburg, MD) encompassing essentially the entire SIV genome. Labeled cells were visualized using fluorescent dyes Alexa 568 (red)-conjugated sheep anti-digoxigenin antibodies. The plasma viral load and cell-associated viral RNA and DNA were measured as we previously described (26). In brief, total RNA or DNA was extracted from plasma or GC Tfh cells sorted from lymph nodes. Reverse transcription (RT) was performed to synthesize cDNA from RNA samples using the commercial kit (Cat. # 18080044. ThermoFisher Scientific). Amplification and detection of SIV DNA/RNA were determined by TaqMan real-time PCR (ABI 7900HT sequence detection system, Life Techologies) targeting conservative region of SIV gag with SIV-specific primer and probe (38). Program was run with a 40 cycles at 95°C for 15 seconds and 60°C for 1 minute. Viral copy numbers were determined by plotting Cycle quantification (Cq) values obtained from unknown (i.e. test) samples against the exogenous calibration curves generated from known amounts of RNA or DNA standard, and finally normalized by known copies of spiked RNA or cell numbers.

Plasma cytokines/chemokines quantification, viral p27 antigen and anti-SIV gp120 measurement

Proinflammatory cytokines in plasma were measured by Luminex 200 sytems (Bio-Rad Inc., Hercules, CA, USA) according to the manufacturer's instructions. Prior to assays, plasma samples were thawed and centrifuged. Cytokine levels were measured using the ProcartaPlex NHP cytokine/GF37plex (Invitrogen) according to manufacturer's instructions. The reactions in microtiter plates were read on a Bioplex-200 system instrument and results were calculated using BioPlex software version 6 (BioRad, Hercules, CA). Plasma p27 and anti-SIV gp120 were measured with standard ELISA (p27 ELISA kit, Zeptometrix Corp., Buffalo, NY; native SIV gp120, ABL, Rockville, MD).

Statistics

Statistical analyses were performed using a non-parametric Mann-Whitney *t* test (two tailed) and GraphPad Prism 4.0 software (GraphPad Software, SanDiego, CA). The data are presented as the mean +/− standard error of the mean (s.e.m.) and P values <0.05 were considered statistically significant.

Results

B-cell follicle formation and GC Tfh cell development in lymph nodes of neonatal macaques with age

In developing neonates, lymphoid follicles and germinal center structures are essentially absent at birth, but these structures rapidly develop within the first month of life, as indicated by detection of CD20+ B cell follicles and well organized lymphoid follicle and distinct GC formation clearly visible within the first few weeks of age. Accordingly, very few PD-1high cells were detected in lymph nodes at birth, consistent with the absence of GC at this stage (Fig. 1A). However, Tfh cells rapidly increase in follicles with age in normal infants (Figs. 1B and1C), accompanied by lymphoid follicle formation, and persistent elevation of CXCL13 in plasma through 21 days after birth (Fig. 1D). As shown in Fig. 1E, GC Tfh

(CXCR5+PD-1high CD4+ T) cells in lymph nodes were rare in newborn lymph nodes (~0.25%), but rapidly increased within 1–4 weeks of age, and reached “normal” adult levels (2~6%) after the first month. Similar changes were observed in other lymphoid tissues such as the spleen and gut associated lymphoid tissues (colon) of normal infants. These data suggest that fully functional lymphoid tissues are rapidly established within the first few weeks of normal neonatal development.

Sustained viremia and virus-infected cells in lymph nodes of SIV-infected neonatal macaques

High sustained plasma viral loads are observed in infants infected with SIV at birth, compared with SIV-infected adults in which plasma viral loads “peak” 12–14 days post SIV infection, and then decline to a lower viral “set point” within 2–3 months of infection (4, 39, 40). To explore the effects of immune development on viremia and virus control in SIV-infected neonates, we compared plasma viral loads and SIV RNA+ cells in lymph nodes of infants infected with SIV within 24 hours of birth, to those infected at 4-months of age. In contrast to infants infected with the identical stock and dose at 4-months of age, marked numbers of SIV RNA+ cells in lymph nodes were detected in lymph nodes of neonates infected at birth, as SIV-infected cells emerged at 7 dpi, and their numbers continually expanded throughout the entire lymph node through the development of AIDS, including in the follicles, interfollicular region, paracortex, and medulla (Fig. 2A). Measurements of proviral DNA and SIV RNA in sorted GC Tfh cells from SIV-infected infants at day 21 post SIV infection showed these cells were heavily infected, and the levels of SIV-DNA and -RNA in GC Tfh in the infants infected at birth are equivalent to those infected in adults (Fig. 2D), verifying that lymphoid tissues are also major sites for HIV/SIV infection and replication in infants (41). These infants also had sustained high viremia, with no apparent “set point”, compared with infants infected at 4 months of age or adults post SIV infection, in which a clear peak of SIV RNA and p27 antigens occurs in plasma around day 14, followed by a decline and establishment of a lower viral “set point”, similar to SIV infection in adults (42, 43) (Fig. 2B and2C). This age-dependent difference in viremia demonstrated that even 4 month-old infants demonstrate better virologic control compared to newborns, suggesting the pediatric immune system rapidly develops to generate effective immune responses soon after birth (44). Thus, establishment of functional pediatric immune responses in the first few weeks of neonatal development may be critical for protection from infection by vaccination.

Impairment of GC Tfh cell development, B-cell proliferation and differentiation in SIV-infected neonatal macaques

As shown in Fig.1, lymphoid follicles were rapidly formed in lymph nodes of normal developing neonates in the first few weeks of birth, accompanied by increased numbers of PD-1high cells. To investigate the effects of SIV infection on GC Tfh cells of neonates, we compared the dynamics of CXCR5+PD-1high CD4+ T-cells (GC Tfh), CD20+ B-cells, B-cell proliferation and B-cell differentiation in lymph nodes of SIV-infected and age-matched normal neonates. Immunohistochemistry demonstrated that in normal (uninfected) infants, CD20+ B cells in lymph nodes rapidly increased with age, and aggregated to form distinct follicles, containing progressively increasing numbers of PD-1+ cells in the center of

follicles which were clearly distinguishable by 7 days of age (Fig. 3A). In stark contrast, PD-1+ cell populations were essentially absent in lymph nodes of any SIV-infected neonates, accompanied by severely impaired lymphoid follicle development (Figs. 3A and B). Histological assessments clearly showed that follicle structure formation was disrupted in all SIV-infected infants (Fig. 3C). In normal developing infants, 80% of lymphoid follicles were secondary, having prominent germinal centers with light and dark zones, and a thick paracortex densely packed with small lymphocytes in the lymph nodes of SIV naïve infants by 21 to 90 days of age (Fig. 3C). In contrast, numbers of follicles were markedly decreased in age-matched infants post SIV infection, and identifiable follicles completely lacked germinal center formation (Fig. 3D). In all infants that were euthanized after 30 days of infection, there was severe to complete disruption of lymph node follicular architecture. Most infants euthanized due to disease progression had massive T and B cell depletion, disruption of follicular architecture, and hypocellular, dilated medullary sinuses (sinus ectasia) and thickened medullar cords lined with hypertrophic endothelial cells. Sinuses also contained increased numbers of band cells, all consistent chronic, aberrant, immune stimulation with terminal lymphoid depletion/exhaustion. Flow cytometry of LN cell suspensions also indicated marked an absence of GC Tfh cells in SIV-infected infants (Fig. 4A). In contrast, there were no significant changes in frequencies of CD20+ B cells in lymph nodes between SIV-infected and SIV naïve age-matched infants (Fig. 4B) this was likely due to the equal depletion of other cell subsets in these preparations, as B cells were clearly depleted in lymphoid tissues of all SIV-infected infants by immunohistochemistry (Fig. 3D). Further, LN B cells of SIV-infected infants showed significantly reduced levels of B-cell proliferation as indicated by lower levels of Ki67+ B-cells, which are the dominant subset among germinal center B cells of naïve, uninfected infants (45) (Fig. 4C). Resting memory B-cells (IgD+CD27+) also decreased in lymph nodes of infected infants compared to age-matched controls (Fig. 4D), which corresponded with markedly increased levels of memory B cell (IgD-CD27+) generation in infected infants. Note that at 14 dpi (peak viremia) memory B cells (IgD-CD27+) were already significantly increased in infected neonates (Fig. 4E). Consistent with lower numbers of GC Tfh cells, and the reduced B cell proliferation in lymph nodes, levels of plasma anti-SIV gp120 in SIV-infected infants were also significantly lower than SIV+ adults after 3 months of SIV infection (Fig. 4F), suggesting humoral immune responses in HIV/SIV-infected infants were severely impaired, especially when compared to SIV-infected adults. These findings indicate that SIV infection of neonates at birth results in markedly compromised lymphoid follicle formation, impaired GC Tfh cell development, and subsequent severe defects in B-cell differentiation, proliferation, and maturation.

Limited proinflammatory responses in SIV-infected neonatal macaques

Prior studies have shown a “cytokine storm” is induced in acute SIV infection of adult macaques (46) and HIV-infected humans (47, 48), and the proinflammatory cytokines produced may contribute to altered development and differentiation of GC Tfh cells, and over-activity of GC in pathologic conditions (26). Here we analyzed levels of plasma proinflammatory cytokines in neonatal animals infected with SIV at birth. In contrast to SIV-infected adults, proinflammatory cytokine responses were not significantly increased in SIV infected infants compared to age-matched normal controls. In fact, samples compared

from naïve infants 2–3 months of age consistently showed higher constitutive levels of several pro-inflammatory cytokines compared to SIV-infected infants (Fig. 5). This suggests In addition to other effects of SIV, this lack of proinflammatory responses in neonates post HIV/SIV infection may play a causative role in the lack of lymphoid follicle, germinal center, reaction, as well as Tfh cell development and maturation, resulting in pathogen-specific unresponsiveness, clonal anergy/tolerance, and more rapid disease progression in pediatric HIV infection.

Discussion

T follicular helper (Tfh) cells play an essential role in B-cell proliferation, differentiation, and generating antigen-specific antibody responses. Here we compared B-cell follicle formation and GC Tfh and B cell development in germinal centers of normal and SIV-infected neonates *in situ*. The results indicate that lymph node follicles are rapidly formed in the first few weeks of birth, accompanied with increases GC Tfh cells with age. However, SIV infection in neonates at birth essentially prevented the development and differentiation of germinal centers and GC Tfh and B-cells, as indicated by markedly lower levels of GC Tfh cells in lymph nodes, reduced B-cell proliferation and differentiation, and limited proinflammatory cytokine responses throughout SIV infection, compared with age-matched controls. Thus HIV/SIV infection in neonates clearly leads to rapid impairment of lymph node structural, and functional development, preventing normal maturation of the humoral immune system. These early immunologic deficits likely contribute to the sustained high viremia, and rapid disease progression typical of pediatric AIDS.

The systemic immune system of infants is relatively immature, with few to no mature memory cells, and infants typically do not respond as well to systemic infections as adults (3, 49). In fact over 3 million neonatal deaths per year are attributed to various infectious diseases (50). The maturation of the immune system in neonates is partially controlled by environmental and intrinsic factors (51–53), as evidenced by changes in phenotype and numbers of neonatal Tfh and B-cells in response to different environments (53–55). In developing neonates, B cell follicles are rapidly formed in the first few days to weeks of birth, concomitant with increased numbers of GC Tfh cells that reside within GCs of follicles (Fig.1). It is reported the chemoattractant CXCL13 plays a central role in homing of Tfh and B cells (56), and in organizing both B-cell follicles and GCs in lymphoid tissues (57, 58). Thus plasma levels of CXCL13 play a role in the generation of neutralizing antibodies (nAbs) and may be used as a biomarker of GC activity (59). As shown in Fig. 1D, levels of plasma CXCL13 gradually increased through the first 21 days of age in normal infants, consistent with the timing of follicle formation and the peak of GC Tfh cells in LNs (Figs. 4A). However, the levels of plasma CXCL13 decreased afterwards, probably correlating with sufficient GC induction and maturation to antigens exposed after birth. These findings suggest the immune system rapidly develops in the early life of neonates to facilitate neonatal immune maturation and host immunity. To compare host immunity in developing neonates, we compared levels of plasma viral RNA and viral antigen (p27) in animals that were inoculated by SIV at birth to those infected at 4-months of age. The results showed that neonatal macaques maintained high viremia post SIV infection at birth, compared with infants infected later who showed a clear viral “peak” and subsequent lower

"set point" (Fig. 2). In fact, the dynamics of viremia in infants infected at 4 months of age to those of adults. Although it has been reported that bNabs are observed in HIV-infected children (2), this does not appear to result in better containment of infection in infants without therapy. Notably, the levels of plasma p27 showed some differences compared to plasma viral load between SIV-infected cohorts (43, 60), probably reflecting higher and earlier viral replication, and delayed viral protein clearance due to immature immune systems in HIV/SIV-infected infants. Consistent with this, studies of human infants that distinguished in utero, intrapartum and postnatal infection show median survival times from infection of 208, 380, and >500 days respectively (61). Combined, these data demonstrate the neonatal immune system rapidly develops with age to defend against potential pathogens encountered soon after birth.

In T-cell dependent (primary) antibody responses, Tfh cells fine-tune B-cell development through the release of specific cytokines that trigger B cell expansion and differentiation as well as through direct yet intermittent cell-to cell interactions between GC Tfh and B cells within GC. These interactions eventually result in full somatic hypermutation of germline antibody genes, and expanded Ig repertoires with nAb potential (19–21, 62). Neonatal B cells display a naïve phenotype with only a partially developed repertoire of surface immunoglobulins, thus their capacity for generating antibodies is limited. However, our results clearly showed that SIV infection in newborns delayed formation of follicles and GC structures, albeit we detected no changes in percentages of total CD20+ B cells in lymph nodes (Fig. 4B). Importantly, very few GC Tfh cells were detected in lymph nodes of SIV-infected neonatal macaques throughout SIV infection compared with their rapid development and progressive increase in age-matched controls (Figs. 3 and Fig. 4A). We recently reported that persistent HIV/SIV infection results in expansion of GC Tfh cells in chronic SIV infection of adult macaques (26), which correlated with higher viremia (63). This is in stark contrast to the significant reduction of GC Tfh cells observed in SIV-infected infants here, which may be the result of limited or persistent proinflammatory responses to infection (Fig. 5) or potentially other yet unknown factors. In addition, frequencies of both proliferating (Ki-67+) B cells, (representing functional GC B-cells), and resting memory B cells in lymph nodes are also significantly lower in SIV-infected infants than controls (Figs. 4C and4D), indicating differentiation of B-cells is also severely impaired in SIV-infected neonatal macaques. Although total memory B cells in lymph nodes increased in acute infection (day 14) (Fig. 4E), accompanying peak viremia, likely probably reflecting expansion of short-lived memory B cell differentiation responding to viral antigens yet these were not sustained thereafter, reflecting lack of GC Tfh cell help. These findings are consistent with other reports showing decreased frequency and number of resting memory B cells, and increased percentages of switched memory B cells are in HIV-infected children (64, 65). Further, persistent B-cell defects are often observed in HIV-infected children, as indicated by subclinical immune abnormalities and defective B-cell maturation in HIV-1-infected children even when receiving antiretroviral therapy (ART) from birth (65–68). We propose that the damage to B-cell development in SIV-infected neonates occurs early, and is mainly attributed to direct infection and dysregulation of Tfh cells (Fig. 2D), resulting in impaired B cell maturation. This is supported by reports of impaired Tfh cells which correlate with lower levels of B-cell differentiation, including reduced BCR/co-stimulatory

signaling, and lower frequencies of resting memory B cells in HIV infected children (53, 65). Indeed, Tfh cell loss or dysfunction during HIV infection impairs B-cell responses to HIV in adults (30), and in HIV+ children, it even impairs their responses to other vaccines (69). It is known that the safety and effectiveness of vaccines in HIV-infected children varies with age at vaccination and their immune status. For example, infants with symptomatic HIV infection should not receive live attenuated vaccine such as attenuated BCG and yellow fever vaccine. In general, antibody responses to vaccines are lower in HIV-infected children than age-matched uninfected children, albeit occasionally protective levels to some vaccines develop. However, HIV-infected children who do respond to vaccines also have a more rapid decline in antibody titres than uninfected children (70, 71). Thus, strategies for treatment and vaccination should be optimized for HIV-infected infants after initiation of ART (72).

Combined, we hypothesize HIV infection of neonates compromises humoral immune responses with regard to breadth, magnitude and specificity, all due to impairment of organized lymphoid tissue development and loss of Tfh cells. Although it has been reported that bNabs are observed in HIV-infected children (2), this does not appear to result in better containment of infection in infants without therapy. We and others previously reported that persistent SIV infection in adults is responsible for differentiation and aberrant expansion of GC Tfh cells in lymph nodes mediated through the production and elevation of proinflammatory cytokines including IL-4, IL-6 and IFN-γ (19, 26, 73–80). Here we examined the levels of plasma proinflammatory cytokines in SIV-infected neonatal macaques, and compared their levels with age-matched controls. However, as indicated in Fig. 5, SIV infection of neonates did not induce significant increases in proinflammatory responses in the first several weeks of infection, which is in stark contrast to the “cytokine storm” rapidly induced in SIV-infected adults (46). Since cytokines, especially IL-4 and IL-6, play major roles in the differentiation and localization of Tfh cells in GC of neonatal lymphoid tissues and B-cell function (65, 81), the lower levels of proinflammatory responses in neonates may play a role in the lack of GC Tfh development in acute stages of SIV infection. Notably, there were no significant differences in levels of proinflammatory cytokines between SIV naïve and SIV-infected infants until 3 months age. Thus, these particular proinflammatory cytokines may not be dominant factors in the initial GC Tfh cell development and differentiation, but likely play a role afterwards. The cellular and molecular mechanisms behind GC Tfh cell development and differentiation, especially in neonates needs to be further investigated.

In conclusion, HIV/SIV infection of neonates prevents the development and differentiation of normal organized lymphoid tissue development, and corresponding generation of GC Tfh cells and mature B cells, resulting in inadequate antibody responses, and rapid disease progression in HIV/SIV-infected neonates. Further understanding of neonatal immunological development may lead to improved treatments for combatting pediatric AIDS and other infectious diseases of infants and children.

ACKNOWLEDGEMENTS:

We thank Calvin Lanclos and Dawn Szeltner for flow cytometry support and Maury Duplantis and Meagan Watkins for technical support.

This work was supported by NIH grants R01 DE025432, R01 AI099795, S10 OD019964, the National Center for Research Resources, the Office of Research Infrastructure Programs (ORIP) of the National Institutes of Health through grant no. OD011104 and Tulane Bridge Fund Award.

References

1. Simon AK, Hollander GA, McMichael A. 2015 Evolution of the immune system in humans from infancy to old age. Proc Biol Sci 282:20143085. [PubMed: 26702035]
2. Goo L, Chohan V, Nduati R, Overbaugh J. 2014 Early development of broadly neutralizing antibodies in HIV-1-infected infants. Nat Med 20:655–658. [PubMed: 24859529]
3. Wang X, Rasmussen T, Pahar B, Poonia B, Alvarez X, Lackner AA, Veazey RS. 2007 Massive infection and loss of CD4+ T cells occurs in the intestinal tract of neonatal rhesus macaques in acute SIV infection. Blood 109:1174–1181. [PubMed: 17047153]
4. Wang X, Xu H, Pahar B, Alvarez X, Green LC, Dufour J, Moroney-Rasmussen T, Lackner AA, Veazey RS. 2010 Simian immunodeficiency virus selectively infects proliferating CD4+ T cells in neonatal rhesus macaques. Blood 116:4168–4174. [PubMed: 20716768]
5. Zinkernagel RM. 2001 Maternal antibodies, childhood infections, and autoimmune diseases. N Engl J Med 345:1331–1335. [PubMed: 11794153]
6. Okada T, Miller MJ, Parker I, Krummel MF, Neighbors M, Hartley SB, O'Garra A, Cahalan MD, Cyster JG. 2005 Antigen-engaged B cells undergo chemotaxis toward the T zone and form motile conjugates with helper T cells. PLoS Biol 3:e150. [PubMed: 15857154]
7. Qi H, Cannons JL, Klauschen F, Schwartzberg PL, Germain RN. 2008 SAP-controlled T-B cell interactions underlie germinal centre formation. Nature 455:764–769. [PubMed: 18843362]
8. Dal Porto JM, Haberman AM, Kelsoe G, Shlomchik MJ. 2002 Very low affinity B cells form germinal centers, become memory B cells, and participate in secondary immune responses when higher affinity competition is reduced. J Exp Med 195:1215–1221. [PubMed: 11994427]
9. Shih TA, Meffre E, Roederer M, Nussenzweig MC. 2002 Role of BCR affinity in T cell dependent antibody responses in vivo. Nat Immunol 3:570–575. [PubMed: 12021782]
10. Kerfoot SM, Yaari G, Patel JR, Johnson KL, Gonzalez DG, Kleinstein SH, Haberman AM. 2011 Germinal center B cell and T follicular helper cell development initiates in the interfollicular zone. Immunity 34:947–960. [PubMed: 21636295]
11. Kitano M, Moriyama S, Ando Y, Hikida M, Mori Y, Kurosaki T, Okada T. 2011 Bcl6 protein expression shapes pre-germinal center B cell dynamics and follicular helper T cell heterogeneity. Immunity 34:961–972. [PubMed: 21636294]
12. Jacob J, Kelsoe G, Rajewsky K, Weiss U. 1991 Intraclonal generation of antibody mutants in germinal centres. Nature 354:389–392. [PubMed: 1956400]
13. Berek C, Berger A, Apel M. 1991 Maturation of the immune response in germinal centers. Cell 67:1121–1129. [PubMed: 1760840]
14. Crotty S 2011 Follicular helper CD4 T cells (TFH). Annu Rev Immunol 29:621–663. [PubMed: 21314428]
15. Victora GD, Nussenzweig MC. 2012 Germinal centers. Annu Rev Immunol 30:429–457. [PubMed: 22224772]
16. De Silva NS, Klein U. 2015 Dynamics of B cells in germinal centres. Nat Rev Immunol 15:137–148. [PubMed: 25656706]
17. Corcoran LM, Tarlinton DM. 2016 Regulation of germinal center responses, memory B cells and plasma cell formation-an update. Curr Opin Immunol 39:59–67. [PubMed: 26799208]
18. Gatto D, Brink R. 2010 The germinal center reaction. J Allergy Clin Immunol 126:898–907; quiz 908–899. [PubMed: 21050940]
19. Weinstein JS, Herman EI, Lainez B, Licona-Limon P, Esplugues E, Flavell R, Craft J. 2016 TFH cells progressively differentiate to regulate the germinal center response. Nat Immunol 17:1197–1205. [PubMed: 27573866]
20. Wang Y, Shi J, Yan J, Xiao Z, Hou X, Lu P, Hou S, Mao T, Liu W, Ma Y, Zhang L, Yang X, Qi H. 2017 Germinal-center development of memory B cells driven by IL-9 from follicular helper T cells. Nat Immunol 18:921–930. [PubMed: 28650481]

21. Zhang TT, Gonzalez DG, Cote CM, Kerfoot SM, Deng S, Cheng Y, Magari M, Haberman AM. 2017 Germinal center B cell development has distinctly regulated stages completed by disengagement from T cell help. Elife 6.
22. Blink EJ, Light A, Kallies A, Nutt SL, Hodgkin PD, Tarlinton DM. 2005 Early appearance of germinal center-derived memory B cells and plasma cells in blood after primary immunization. J Exp Med 201:545–554. [PubMed: 15710653]
23. Shulman Z, Gitlin AD, Weinstein JS, Lainez B, Esplugues E, Flavell RA, Craft JE, Nussenzweig MC. 2014 Dynamic signaling by T follicular helper cells during germinal center B cell selection. Science 345:1058–1062. [PubMed: 25170154]
24. Reinhardt RL, Liang HE, Locksley RM. 2009 Cytokine-secreting follicular T cells shape the antibody repertoire. Nat Immunol 10:385–393. [PubMed: 19252490]
25. Xu H, Wang X, Lackner AA, Veazey RS. 2014 PD-1(HIGH) Follicular CD4 T Helper Cell Subsets Residing in Lymph Node Germinal Centers Correlate with B Cell Maturation and IgG Production in Rhesus Macaques. Front Immunol 5:85. [PubMed: 24678309]
26. Xu H, Wang X, Malam N, Aye PP, Alvarez X, Lackner AA, Veazey RS. 2015 Persistent Simian Immunodeficiency Virus Infection Drives Differentiation, Aberrant Accumulation, and Latent Infection of Germinal Center Follicular T Helper Cells. J Virol 90:1578–1587. [PubMed: 26608323]
27. Wang X, Ziani W, Xu H. 2016 Changes in Follicular CD4+ T Helper Cells as a Marker for Evaluating Disease Progression in the Competition between HIV and Host Immunity. Front Immunol 7:474. [PubMed: 27843442]
28. Perreau M, Savoye AL, De Crignis E, Corpataux JM, Cubas R, Haddad EK, De Leval L, Graziosi C, Pantaleo G. 2013 Follicular helper T cells serve as the major CD4 T cell compartment for HIV-1 infection, replication, and production. J Exp Med 210:143–156. [PubMed: 23254284]
29. Overbaugh J, Morris L. 2012 The Antibody Response against HIV-1. Cold Spring Harb Perspect Med 2:a007039. [PubMed: 22315717]
30. Cubas RA, Mudd JC, Savoye AL, Perreau M, van Grevenynghe J, Metcalf T, Connick E, Meditz A, Freeman GJ, Abesada-Terk G, Jr., Jacobson JM, Brooks AD, Crotty S, Estes JD, Pantaleo G, Lederman MM, Haddad EK. 2013 Inadequate T follicular cell help impairs B cell immunity during HIV infection. Nat Med 19:494–499. [PubMed: 23475201]
31. Amu S, Ruffin N, Rethi B, Chiodi F. 2013 Impairment of B-cell functions during HIV-1 infection. AIDS 27:2323–2334. [PubMed: 23595152]
32. Kardava L, Moir S, Shah N, Wang W, Wilson R, Buckner CM, Santich BH, Kim LJ, Spurlin EE, Nelson AK, Wheatley AK, Harvey CJ, McDermott AB, Wucherpfennig KW, Chun TW, Tsang JS, Li Y, Fauci AS. 2014 Abnormal B cell memory subsets dominate HIV-specific responses in infected individuals. J Clin Invest 124:3252–3262. [PubMed: 24892810]
33. Mouquet H 2014 Antibody B cell responses in HIV-1 infection. Trends Immunol 35:549–561. [PubMed: 25240985]
34. Goulder PJ, Lewin SR, Leitman EM. 2016 Paediatric HIV infection: the potential for cure. Nat Rev Immunol 16:259–271. [PubMed: 26972723]
35. DeMaria MA, Casto M, O'Connell M, Johnson RP, Rosenzweig M. 2000 Characterization of lymphocyte subsets in rhesus macaques during the first year of life. Eur J Haematol 65:245–257. [PubMed: 11073165]
36. Xu H, Wang X, Liu DX, Moroney-Rasmussen T, Lackner AA, Veazey RS. 2012 IL-17-producing innate lymphoid cells are restricted to mucosal tissues and are depleted in SIV-infected macaques. Mucosal Immunol 5:658–669. [PubMed: 22669579]
37. Xu H, Wang X, Pahar B, Moroney-Rasmussen T, Alvarez X, Lackner AA, Veazey RS. 2010 Increased B7-H1 expression on dendritic cells correlates with programmed death 1 expression on T cells in simian immunodeficiency virus-infected macaques and may contribute to T cell dysfunction and disease progression. J Immunol 185:7340–7348. [PubMed: 21059890]
38. Monjure CJ, Tatum CD, Panganiban AT, Arainga M, Traina-Dorge V, Marx PA, Jr., Didier ES. 2014 Optimization of PCR for quantification of simian immunodeficiency virus genomic RNA in plasma of rhesus macaques (Macaca mulatta) using armored RNA. J Med Primatol 43:31–43. [PubMed: 24266615]

39. Palumbo PE, Raskino C, Fiscus S, Pahwa S, Fowler MG, Spector SA, Englund JA, Baker CJ. 1998 Predictive value of quantitative plasma HIV RNA and CD4+ lymphocyte count in HIV-infected infants and children. JAMA 279:756–761. [PubMed: 9508151]
40. De Rossi A, Masiero S, Giaquinto C, Ruga E, Comar M, Giacca M, Chieco-Bianchi L. 1996 Dynamics of viral replication in infants with vertically acquired human immunodeficiency virus type 1 infection. J Clin Invest 97:323–330. [PubMed: 8567951]
41. Estes JD, Kityo C, Ssali F, Swainson L, Makamdop KN, Del Prete GQ, Deeks SG, Luciw PA, Chipman JG, Beilman GJ, Hoskuldsson T, Khoruts A, Anderson J, Deleage C, Jasurda J, Schmidt TE, Hafertepe M, Callisto SP, Pearson H, Reimann T, Schuster J, Schoephoerster J, Southern P, Perkey K, Shang L, Wietgrefe SW, Fletcher CV, Lifson JD, Douek DC, McCune JM, Haase AT, Schacker TW. 2017 Defining total-body AIDS-virus burden with implications for curative strategies. Nat Med 23:1271–1276. [PubMed: 28967921]
42. Merino KM, Allers C, Didier ES, Kuroda MJ. 2017 Role of Monocyte/Macrophages during HIV/SIV Infection in Adult and Pediatric Acquired Immune Deficiency Syndrome. Front Immunol 8:1693. [PubMed: 29259605]
43. Fultz PN, McGinn T, Davis IC, Romano JW, Li Y. 1999 Coinfection of macaques with simian immunodeficiency virus and simian T cell leukemia virus type I: effects on virus burdens and disease progression. J Infect Dis 179:600–611. [PubMed: 9952366]
44. Tobin NH, Aldrovandi GM. 2013 Immunology of pediatric HIV infection. Immunol Rev 254:143–169. [PubMed: 23772619]
45. Fan W, Demers AJ, Wan Y, Li Q. 2018 Altered Ratio of T Follicular Helper Cells to T Follicular Regulatory Cells Correlates with Autoreactive Antibody Response in Simian Immunodeficiency Virus-Infected Rhesus Macaques. J Immunol doi:10.4049/jimmunol.1701288.
46. Xu H, Wang X, Morici LA, Pahar B, Veazey RS. 2011 Early divergent host responses in SHIVsf162P3 and SIVmac251 infected macaques correlate with control of viremia. PLoS One 6:e17965. [PubMed: 21464951]
47. Zhang R, Miner JJ, Gorman MJ, Rausch K, Ramage H, White JP, Zuiani A, Zhang P, Fernandez E, Zhang Q, Dowd KA, Pierson TC, Cherry S, Diamond MS. 2016 A CRISPR screen defines a signal peptide processing pathway required by flaviviruses. Nature 535:164–168. [PubMed: 27383988]
48. Stacey AR, Norris PJ, Qin L, Haygreen EA, Taylor E, Heitman J, Lebedeva M, DeCamp A, Li D, Grove D, Self SG, Borrow P. 2009 Induction of a striking systemic cytokine cascade prior to peak viremia in acute human immunodeficiency virus type 1 infection, in contrast to more modest and delayed responses in acute hepatitis B and C virus infections. J Virol 83:3719–3733. [PubMed: 19176632]
49. Basha S, Surendran N, Pichichero M. 2014 Immune responses in neonates. Expert Rev Clin Immunol 10:1171–1184. [PubMed: 25088080]
50. Liu L, Johnson HL, Cousens S, Perin J, Scott S, Lawn JE, Rudan I, Campbell H, Cibulskis R, Li M, Mathers C, Black RE, Child Health Epidemiology Reference Group of WHO, Unicef. 2012 Global, regional, and national causes of child mortality: an updated systematic analysis for 2010 with time trends since 2000. Lancet 379:2151–2161. [PubMed: 22579125]
51. Hodgins DC, Shewen PE. 2012 Vaccination of neonates: problem and issues. Vaccine 30:1541–1559. [PubMed: 22189699]
52. Siegrist CA. 2007 The challenges of vaccine responses in early life: selected examples. J Comp Pathol 137 Suppl 1:S4–9. [PubMed: 17559867]
53. Mastelic B, Kamath AT, Fontannaz P, Tougne C, Rochat AF, Belnoue E, Combescure C, Auderset F, Lambert PH, Tacchini-Cottier F, Siegrist CA. 2012 Environmental and T cell-intrinsic factors limit the expansion of neonatal follicular T helper cells but may be circumvented by specific adjuvants. J Immunol 189:5764–5772. [PubMed: 23162125]
54. Siegrist CA, Aspinall R. 2009 B-cell responses to vaccination at the extremes of age. Nat Rev Immunol 9:185–194. [PubMed: 19240757]
55. Wood N, Siegrist CA. 2011 Neonatal immunization: where do we stand? Curr Opin Infect Dis 24:190–195. [PubMed: 21415741]
56. Mabuka JM, Dugast AS, Muema DM, Reddy T, Ramlakhan Y, Euler Z, Ismail N, Moodley A, Dong KL, Morris L, Walker BD, Alter G, Ndung'u T. 2017 Plasma CXCL13 but Not B Cell

Frequencies in Acute HIV Infection Predicts Emergence of Cross-Neutralizing Antibodies. Front Immunol 8:1104. [PubMed: 28943879]

57. Ansel KM, Ngo VN, Hyman PL, Luther SA, Forster R, Sedgwick JD, Browning JL, Lipp M, Cyster JG. 2000 A chemokine-driven positive feedback loop organizes lymphoid follicles. Nature 406:309–314. [PubMed: 10917533]
58. Allen CD, Okada T, Cyster JG. 2007 Germinal-center organization and cellular dynamics. Immunity 27:190–202. [PubMed: 17723214]
59. Havenar-Daughton C, Lindqvist M, Heit A, Wu JE, Reiss SM, Kendric K, Belanger S, Kasturi SP, Landais E, Akondy RS, McGuire HM, Bothwell M, Vagefi PA, Scully E, Investigators IPCP, Tomaras GD, Davis MM, Poignard P, Ahmed R, Walker BD, Pulendran B, McElrath MJ, Kaufmann DE, Crotty S. 2016 CXCL13 is a plasma biomarker of germinal center activity. Proc Natl Acad Sci U S A 113:2702–2707. [PubMed: 26908875]
60. Ferrantelli F, Rasmussen RA, Buckley KA, Li PL, Wang T, Montefiori DC, Katinger H, Stiegler G, Anderson DC, McClure HM, Ruprecht RM. 2004 Complete protection of neonatal rhesus macaques against oral exposure to pathogenic simian-human immunodeficiency virus by human anti-HIV monoclonal antibodies. J Infect Dis 189:2167–2173. [PubMed: 15181562]
61. Marinda E, Humphrey JH, Iliff PJ, Mutasa K, Nathoo KJ, Piwoz EG, Moulton LH, Salama P, Ward BJ, Group ZS. 2007 Child mortality according to maternal and infant HIV status in Zimbabwe. Pediatr Infect Dis J 26:519–526. [PubMed: 17529870]
62. Zhang Y, Garcia-Ibanez L, Toellner KM. 2016 Regulation of germinal center B-cell differentiation. Immunol Rev 270:8–19. [PubMed: 26864101]
63. Mylvaganam GH, Velu V, Hong JJ, Sadagopal S, Kwa S, Basu R, Lawson B, Villinger F, Amara RR. 2014 Diminished Viral Control during Simian Immunodeficiency Virus Infection Is Associated with Aberrant PD-1hi CD4 T Cell Enrichment in the Lymphoid Follicles of the Rectal Mucosa. J Immunol doi:10.4049/jimmunol.1401222.
64. Muema DM, Macharia GN, Hassan AS, Mwaringa SM, Fegan GW, Berkley JA, Nduati EW, Urban BC. 2015 Control of Viremia Enables Acquisition of Resting Memory B Cells with Age and Normalization of Activated B Cell Phenotypes in HIV-Infected Children. J Immunol 195:1082–1091. [PubMed: 26116511]
65. Bekele Y, Amu S, Bobosha K, Lantto R, Nilsson A, Endale B, Gebre M, Aseffa A, Rethi B, Howe R, Chiodi F. 2015 Impaired Phenotype and Function of T Follicular Helper Cells in HIV-1-Infected Children Receiving ART. Medicine (Baltimore) 94:e1125. [PubMed: 26166114]
66. van den Heuvel D, Driessen GJ, Berkowska MA, van der Burg M, Langerak AW, Zhao D, Charif H, Hartwig NG, van Rossum AM, Fraaij PL, van Dongen JJ, van Zelm MC. 2015 Persistent subclinical immune defects in HIV-1-infected children treated with antiretroviral therapy. AIDS 29:1745–1756. [PubMed: 26372381]
67. Bamford A, Hart M, Lyall H, Goldblatt D, Kelleher P, Kampmann B. 2015 The influence of paediatric HIV infection on circulating B cell subsets and CXCR5(+) T helper cells. Clin Exp Immunol 181:110–117. [PubMed: 25737039]
68. Cotugno N, De Armas L, Pallikkuth S, Rinaldi S, Issac B, Cagigi A, Rossi P, Palma P, Pahwa S. 2017 Perturbation of B Cell Gene Expression Persists in HIV-Infected Children Despite Effective Antiretroviral Therapy and Predicts H1N1 Response. Front Immunol 8:1083. [PubMed: 28955330]
69. Mansoor N, Scriba TJ, de Kock M, Tameris M, Abel B, Keyser A, Little F, Soares A, Gelderbloem S, Mlenjeni S, Denation L, Hawkridge A, Boom WH, Kaplan G, Hussey GD, Hanekom WA. 2009 HIV-1 infection in infants severely impairs the immune response induced by Bacille Calmette-Guerin vaccine. J Infect Dis 199:982–990. [PubMed: 19236280]
70. Moss WJ, Clements CJ, Halsey NA. 2003 Immunization of children at risk of infection with human immunodeficiency virus. Bull World Health Organ 81:61–70. [PubMed: 12640478]
71. Mphahlele MJ, Mda S. 2012 Immunising the HIV-infected child: a view from sub-Saharan Africa. Vaccine 30 Suppl 3:C61–65. [PubMed: 22939024]
72. Cagigi A, Cotugno N, Giaquinto C, Nicolosi L, Bernardi S, Rossi P, Douagi I, Palma P. 2012 Immune reconstitution and vaccination outcome in HIV-1 infected children: present knowledge and future directions. Hum Vaccin Immunother 8:1784–1794. [PubMed: 22906931]

73. Lee SK, Silva DG, Martin JL, Pratama A, Hu X, Chang PP, Walters G, Vinuesa CG. 2012 Interferon-gamma excess leads to pathogenic accumulation of follicular helper T cells and germinal centers. Immunity 37:880–892. [PubMed: 23159227]

74. Maue AC, Eaton SM, Lanthier PA, Sweet KB, Blumerman SL, Haynes L. 2009 Proinflammatory adjuvants enhance the cognate helper activity of aged CD4 T cells. J Immunol 182:6129–6135. [PubMed: 19414765]

75. Jogdand GM, Mohanty S, Devadas S. 2016 Regulators of Tfh Cell Differentiation. Front Immunol 7:520. [PubMed: 27933060]

76. Karnowski A, Chevrier S, Belz GT, Mount A, Emslie D, D'Costa K, Tarlinton DM, Kallies A, Corcoran LM. 2012 B and T cells collaborate in antiviral responses via IL-6, IL-21, and transcriptional activator and coactivator, Oct2 and OBF-1. J Exp Med 209:2049–2064. [PubMed: 23045607]

77. Mauri C, Bosma A. 2012 Immune regulatory function of B cells. Annu Rev Immunol 30:221–241. [PubMed: 22224776]

78. Mitsdoerffer M, Lee Y, Jager A, Kim HJ, Korn T, Kolls JK, Cantor H, Bettelli E, Kuchroo VK. 2010 Proinflammatory T helper type 17 cells are effective B-cell helpers. Proc Natl Acad Sci U S A 107:14292–14297. [PubMed: 20660725]

79. Arkatkar T, Du SW, Jacobs HM, Dam EM, Hou B, Buckner JH, Rawlings DJ, Jackson SW. 2017 B cell-derived IL-6 initiates spontaneous germinal center formation during systemic autoimmunity. J Exp Med 214:3207–3217. [PubMed: 28899868]

80. Cain D, Kondo M, Chen H, Kelsoe G. 2009 Effects of acute and chronic inflammation on B-cell development and differentiation. J Invest Dermatol 129:266–277. [PubMed: 19148216]

81. Debock I, Jaworski K, Chadlaoui H, Delbauve S, Passon N, Twyffels L, Leo O, Flamand V. 2013 Neonatal follicular Th cell responses are impaired and modulated by IL-4. J Immunol 191:1231–1239. [PubMed: 23804713]

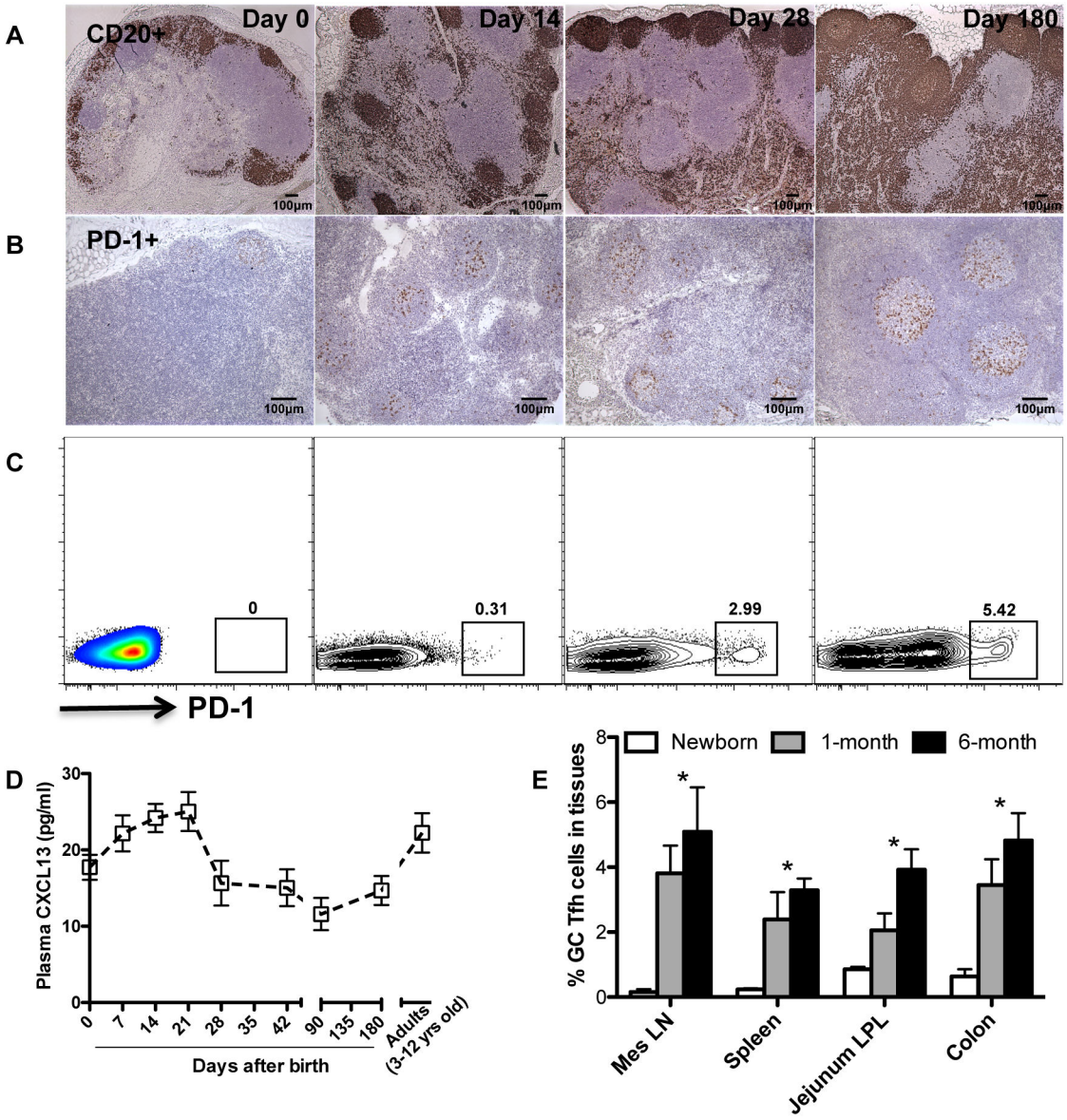

Figure 1. Rapid follicle formation and development of GC Tfh cells in lymph nodes of normal neonatal macaques.

(A) B-cell follicle formation in lymph nodes of normal developing infants as detected by immunohistochemistry for CD20 (B cells); (B) Distribution and dynamics of PD-1 positive cells (Tfh) in germinal centers of lymph nodes of normal neonates with age; (C) Representative flow cytometry dot plots of PD-1high gated CD4+ T cells obtained from lymph nodes of normal infants at 0, 14, 28 and 180 days of age; (D) Levels of plasma CXCL13 in infants with age at day 0 (n=5), 7 (n=3), 14 (n=5), 21 (n=5), 28 (n=4), 42 (n=4), 90 (n=4), 180 (n=5) after birth, compared to adults (n=16). (E) Distribution and localization of GC Tfh cells (CXCR5+PD-1high CD4 T cells) in developing neonates with age showing lymph nodes from newborns (n=5), 1 month (n=4) and 6 months (n=5) after birth. *p<0.05, as compared with newborns. Data are presented as means ± s.e.m (C and D).

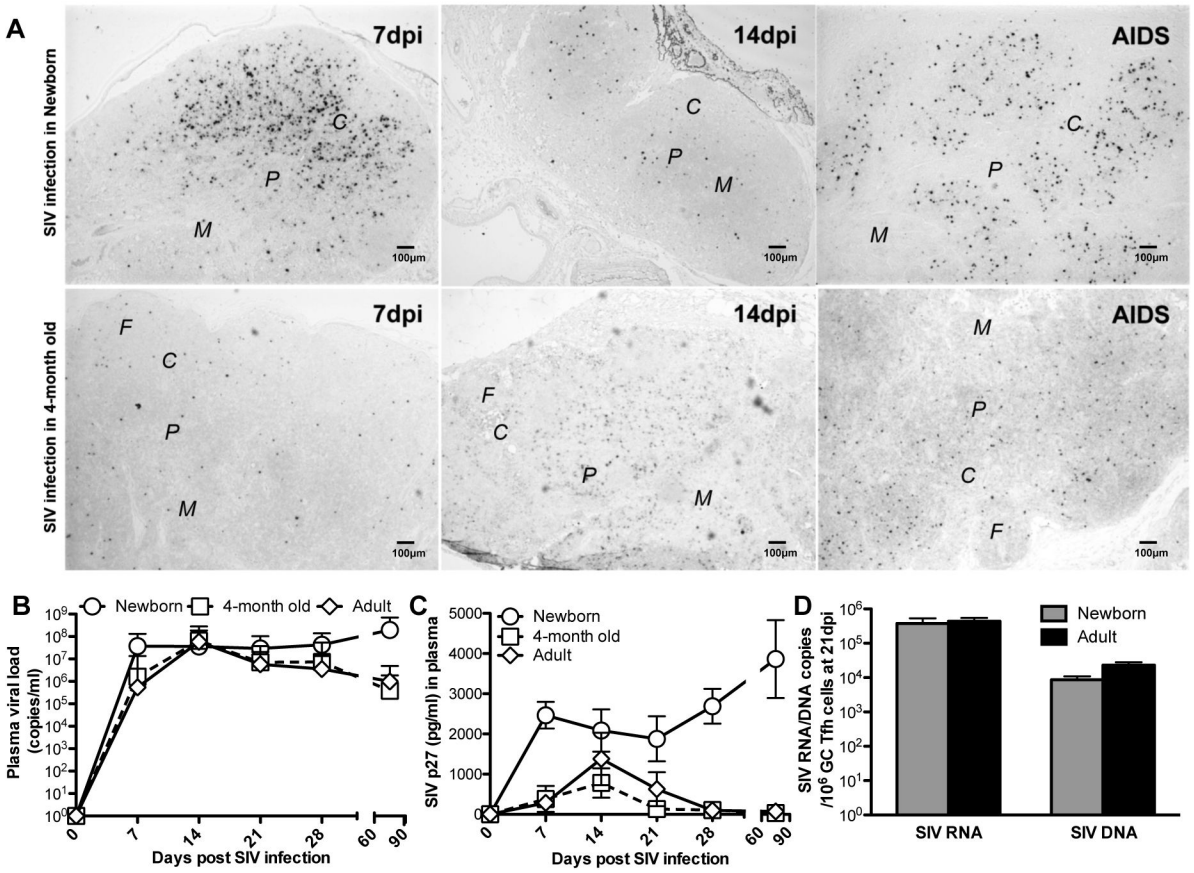

Figure 2. Viral loads and detection of SIV-infected cells in neonatal and infant macaques.

(A) SIV-infected cells in follicle (*F*) cortex (*C*), paracortex (*P*) and medulla (*M*) of lymph nodes of neonatal macaques post SIV infection, as demonstrated by SIV RNA *in situ* hybridization. Levels of plasma viral load (B) and SIV p27 antigen (C) in infants infected with SIV either at birth (n=28), 4-months of age (n=6), or adults (n=12). Note viral loads do not reach a "peak" in infants infected at birth and demonstrate sustained high levels. In contrast, macaques infected at 4 months of age showed declines in viremia after 14 days, and had set points similar to adult infection. $^{*,\#}$ $p<0.05$, compared with SIV naïve newborn (*) or 4-month age/adults (#). (D) Levels of proviral DNA and SIV RNA in sorted GC Tfh cells at day 21 post SIV infection were from the infants at birth (gray bars) or adult (black bars) infected by SIV.

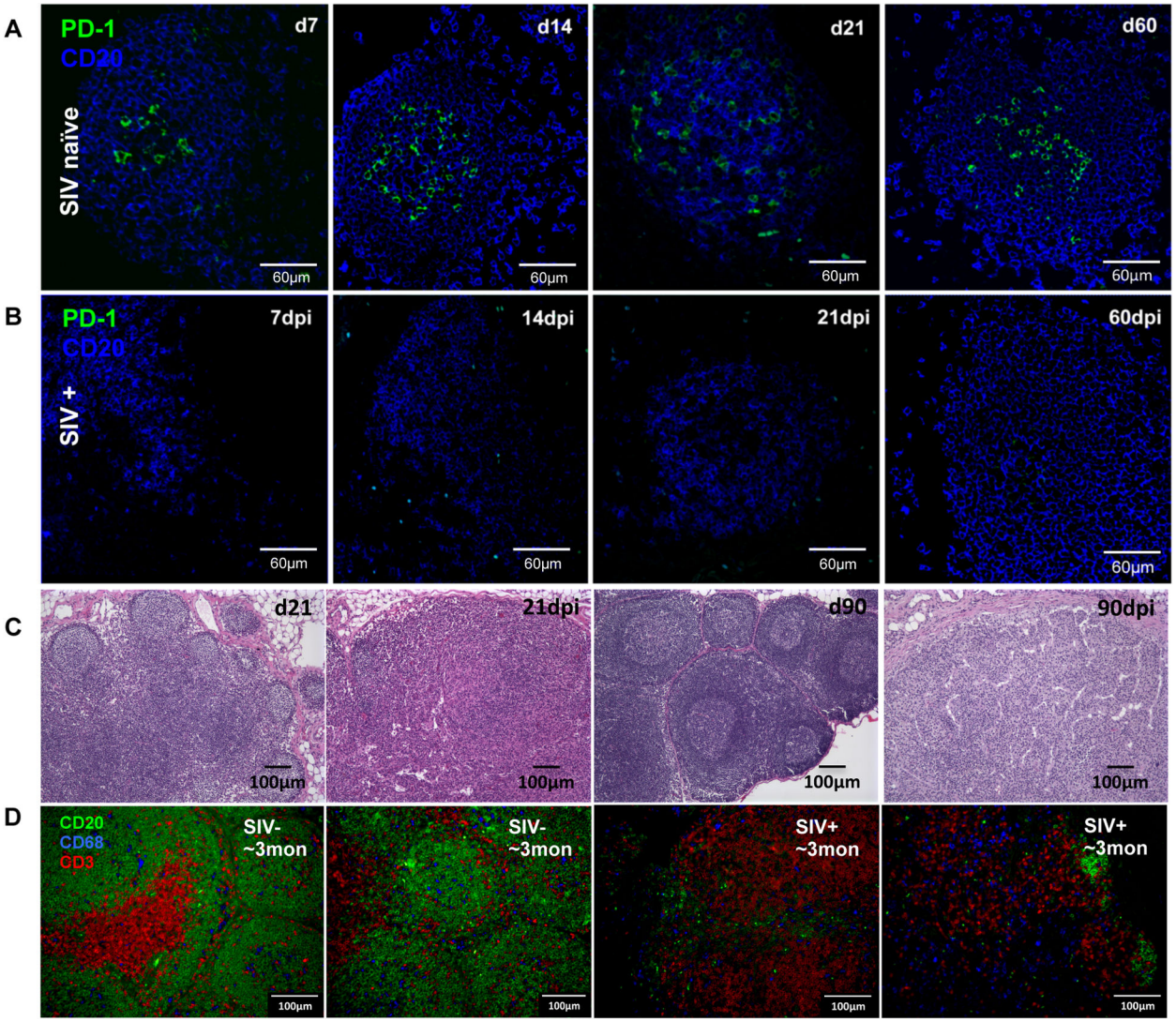

Figure 3. Effects of SIV infection on follicle structure of lymph nodes in neonatal macaques infected with SIVmac251.

Confocal microscopy of PD-1^{+} cells in follicles of lymph nodes in SIV naïve age-matched (A) and SIV-infected neonates post SIV infection (B). CD20, blue; PD-1, green. (C) Histopathological examination of follicles in the lymph nodes of infants with or without SIV infection at birth. The numbers of follicles were decreased and remaining of follicles were primary (lacked germinal center formation) in SIV-infected infants at 21 and 90 dpi, compared with age-matched controls. Severe lymphoid depletion and impaired follicle formation observed throughout SIV infection in infants. All photomicrographs were taken from H&E stained slides at an original magnification of 100×. (D) Confocal image analysis of B/T-cell and macrophages in lymph nodes in SIV naïve or SIV-infected infants with ~3 months age, as shown CD20 (green), CD3 (red) positive cells and macrophage (blue).

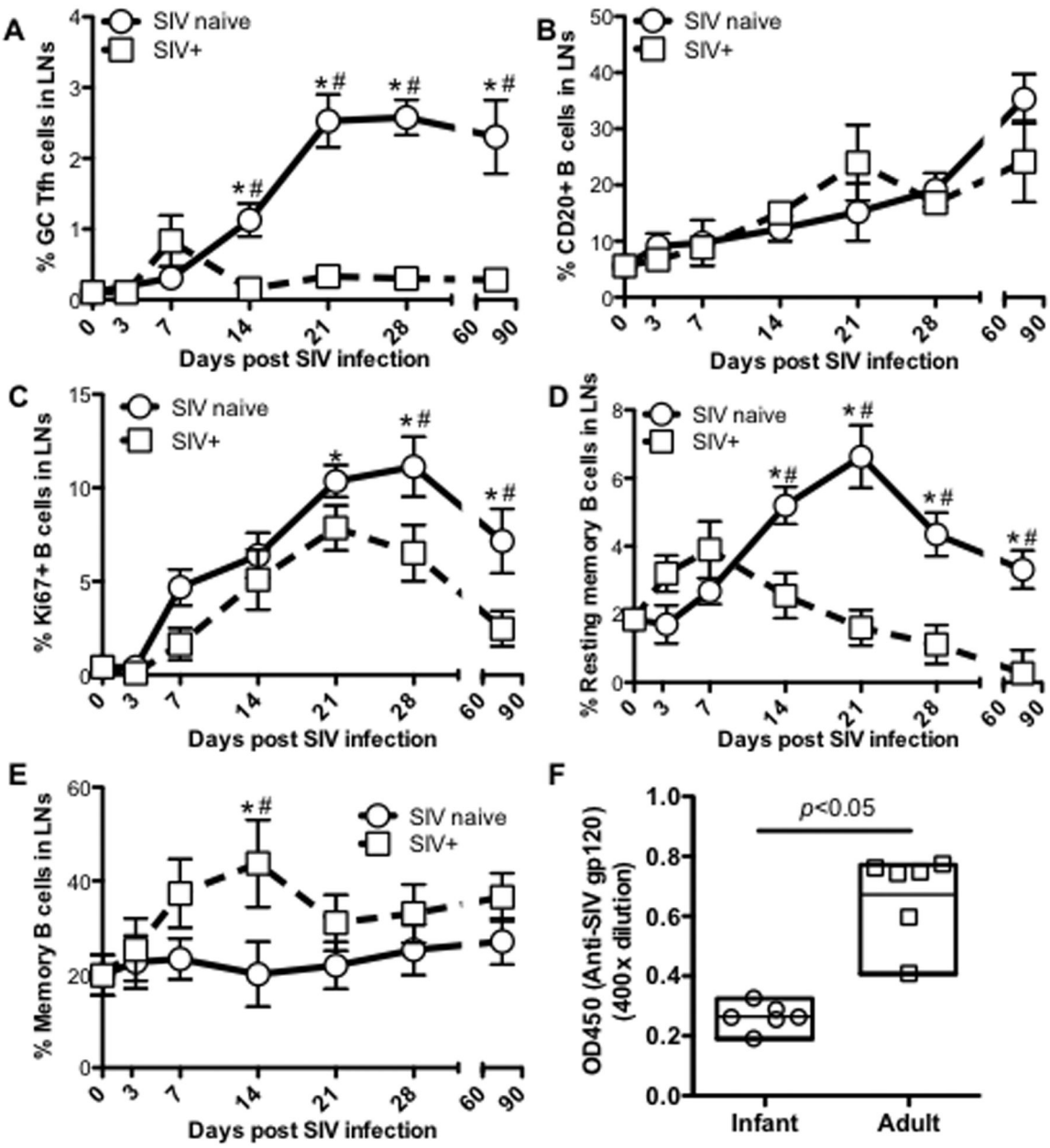

Figure 4. Effects of SIV infection on GC Tfh cell and B-cell differentiation in neonatal macaques infected with SIVmac251.

(A) Changes in GC Tfh cells (CXCR5+PD-1high CD4+ T-cell) in lymph nodes of infants infected with SIV at birth and examined at day 3 (n=3), 7 (n=3), 14 (n=6), 21 (n=5), 28 (n=3) and 2~3 months (n=8) post SIV infection, compared with age-matched uninfected infants (n=35); (B) Percentage of CD20+ B cells in lymph nodes of infants post SIV infection; (C) Proliferation of B cells in lymph nodes of neonates post SIV infection; and (D and E) changes of resting memory B-cell (IgD+CD27+) and memory B-cell in lymph nodes of infants post SIV infection; (F) Levels of plasma anti-SIV gp120 in infants and adults after 3 months SIV infection. *,# $p<0.05$, compared with newborn (*) or age-matched normal infants (#).

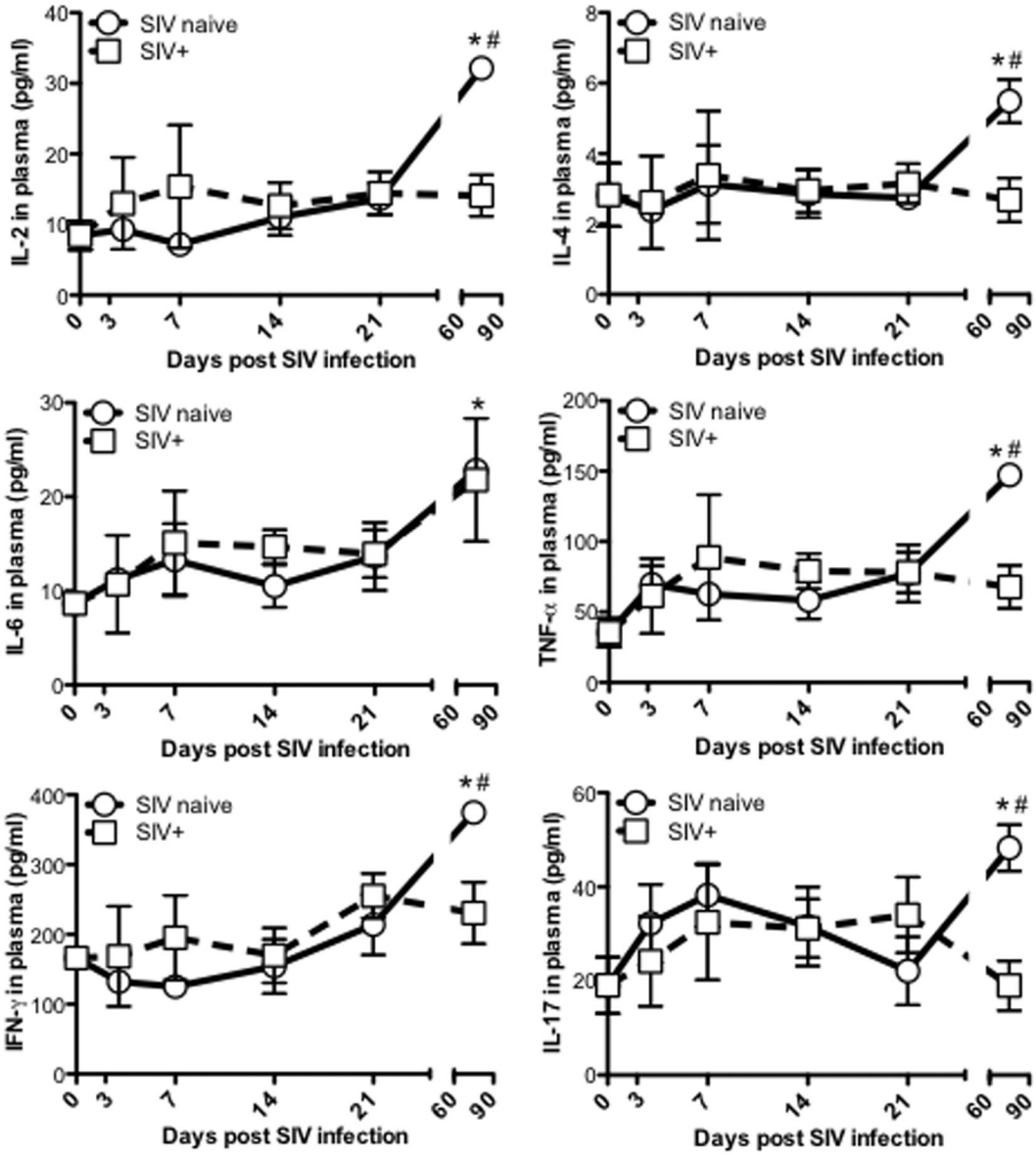

Figure 5. Proinflammatory responses in SIV-infected neonatal macaques.

Levels of plasma proinflammatory cytokines in infants infected with SIV infection at birth (n=28), compared with age-matched uninfected infants (n=35). $^{*,\#}$ $p<0.05$, compared with SIV naïve newborn (*) or age-matched controls (#). Data are presented as mean ± s.e.m.